Environmental Impact Assessment Review 49 (2014) 70–78

Contents lists available at ScienceDirect

Environmental Impact Assessment Review

journal homepage: www.elsevier.com/locate/eiar

# An open source GIS tool to quantify the visual impact of wind turbines and photovoltaic panels

Annalisa Minelli [a], Ivan Marchesini [b,*], Faith E. Taylor [c], Pierluigi De Rosa [d], Luca Casagrande [e], Michele Cenci [f]

[a] Institute Universitaire Européen de la Mer, Université de la Bretagne Occidentale, Rue Dumont D'Urville, 29280 Plouzané, France
[b] National Research Council (CNR), Research Insitute for Geo-hydrological Protection (IRPI), Strada della Madonna Alta 126, 06125 Perugia, Italy
[c] Earth and Environmental Dynamics Research Group, Department of Geography, King's College London, Strand, London WC2R 2LS, United Kingdom
[d] Physics and Geology Department, University of Perugia, Via Zefferino Faina 4, 06123 Perugia, Italy
[e] Gfosservices S.A., Open Source GIS-WebGIS Solutions, Spatial Data Infrastructures, Planning and Counseling, Via F.lli Cairoli 24, 06127 Perugia, Italy
[f] Servizio Energia qualità dell'ambiente, rifiuti, attività estrattive, Regione Umbia, Corso Vannucci 96, 06121 Perugia, Italy

ARTICLE INFO

*Article history:*
Received 30 January 2014
Received in revised form 2 July 2014
Accepted 3 July 2014
Available online xxxx

*Keywords:*
Visual impact
Photovoltaic panels
Wind turbines
Landscape
GRASS GIS

ABSTRACT

Although there are clear economic and environmental incentives for producing energy from solar and wind power, there can be local opposition to their installation due to their impact upon the landscape. To date, no international guidelines exist to guide quantitative visual impact assessment of these facilities, making the planning process somewhat subjective. In this paper we demonstrate the development of a method and an Open Source GIS tool to quantitatively assess the visual impact of these facilities using line-of-site techniques. The methods here build upon previous studies by (i) more accurately representing the shape of energy producing facilities, (ii) taking into account the distortion of the perceived shape and size of facilities caused by the location of the observer, (iii) calculating the possible obscuring of facilities caused by terrain morphology and (iv) allowing the combination of various facilities to more accurately represent the landscape. The tool has been applied to real and synthetic case studies and compared to recently published results from other models, and demonstrates an improvement in accuracy of the calculated visual impact of facilities. The tool is named r.wind.sun and is freely available from GRASS GIS AddOns.



## Introduction

Over the 21st century, global demand for energy is expected to double, arguably requiring growth in renewable energy production such as solar (photovoltaic panel) and wind turbines to reasonably meet demands (Lewis and Nocera, 2006). Although there are clear benefits to these renewable technologies, uptake does not match potential of renewable energy production for a variety of reasons (Painuly, 2001). At a local scale, one such barrier is the aesthetic impact of renewable energy facilities on the landscape (Wüstenhagen et al., 2007). Hence, there is a clear need to carefully locate wind farms and photovoltaic panels to minimise their visual impact and increase social acceptance.

At present, there is not a unilaterally agreed, standardized method to quantify the visual impact of photovoltaic fields and wind farms. Landscape quality evaluations may rely upon local guidelines (Hurtado et al., 2003; Regione Autonoma della Sardegna, 2008), good practice manuals (Landscape Institute, Environmental Management Assessment, 2002; Scottish Natural Heritage et al., 2006; Vissering et al., 2011), survey-based or index methods (Ladenburg, 2009; Tsoutsos et al., 2009), and/or colour and light based methods (e.g., blending with the landscape) (Bishop and Miller, 2007; Chiabrando et al., 2011; Shang and Bishop, 2000).

Typically, the visual impact of a range of environmental phenomena is assessed through viewshed analysis in a GIS. In this method, a digital elevation model is used to determine which parts of the landscape are visible or not visible from a particular vantage point (Longely et al., 2010). For instance, studies have been carried out on the visibility of *Nuraghes* (De Montis and Caschilli, 2012), native buildings from the Isle of Sardinia in Italy, on the visibility of electric transmission towers (Turnbull and Gourlay, 1987), and on the maximisation of the scenic viewpoints along a touristic road (Chamberlain and Meitner, 2013). Manchado et al. (2013) recently reviewed computer programmes available to perform visibility analysis for a variety of purposes.

Visibility analysis techniques have been applied to evaluate solar panel and wind turbine visibility (e.g. Moeller, 2006 and the references therein). We build upon this work by taking into account how the perceived size and shape of an object become distorted depending on the viewing point. An object's shape distortion as perceived by a human eye can affect the quantification of the area affected by visual impact on landscape perception, as we demonstrate.

* Corresponding author.
*E-mail addresses:* Annalisa.Minelli@univ-brest.fr (A. Minelli), Ivan.Marchesini@irpi.cnr.it (I. Marchesini), Faith.Taylor@kcl.ac.uk (F.E. Taylor), Pierluigi.Derosa@unipg.it (P. De Rosa), Luca.Casagrande@gfosservices.it (L. Casagrande), mcenci@regione.umbria.it (M. Cenci).

http://dx.doi.org/10.1016/j.eiar.2014.07.002
0195-9255/

This method is based on the concepts of (i) visibility analysis (Manchado et al., 2013) and visual magnitude (Chamberlain and Meitner, 2013), (ii) human eye perception and its field of view (Costella, 1992; Spector, 1990) and (iii) descriptive geometry (De Rubertis, 1979).

Quantitative analysis of visual impact is performed by (i) computing the field of view of an observer at a specific distance, (ii) evaluating the object shape distortion perceived by a human eye, and (iii) analysing the mutual relation between object, observer and earth morphology. The tool is developed as an add-on module for GRASS GIS, an Open Source GIS software (Neteler and Mitasova, 2008). As the code is completely available, users can freely read, verify, redistribute and modify the code, meaning that the tool is flexible and that the reproducibility of results is guaranteed (Ince et al., 2012).

## Material and methods

The tool developed is named "r.wind.sun". It is coded in the Python programming language (Van Rossum and Drake, 2001) as an add-on module to GRASS GIS, an Open Source GIS software (Neteler and Mitasova, 2008). The tool builds upon the existing GRASS GIS tool "r.viewshed" (Toma et al., 2012) which is based on the concept of line of sight (LOS), the straight line between the observer and object (e.g., Molina-Ruiz et al., 2011).

In the r.wind.sun tool, visual impact is quantified by the proportion of the field of view that is obstructed by the wind turbine or photovoltaic panel. This builds upon previous work by Rodrigues et al. (2010) that measures visual impact as the size of the observed object and half of the full solid angle multiplied by the square of the distance between the object and the observer.

In this section we introduce the key concepts applied to (i) calculate the field of view, (ii) calculate the perceived size of objects within the field of view and (iii) calculate the ratio between the perceived size of object and the field of view and demonstrate that this is independent of distance. In the section Visual impact index, we define the visual impact index and then show the development of the tool to measure this.

### *The human field of view*

In this section we define the shape and size of the region that can be seen by an observer, this is the human field of view (FOV). The "static" FOV is defined by three angles (Fig. 1):

- nasal ($n$): measuring 85°, starting from the nose of the observer and extending outwards across a horizontal plane (Fig. 1a).
- superior ($s$): vertical angle, measuring 65°, starting from the nose of the observer and extending upwards (Fig. 1b).
- inferior ($i$): vertical angle, measuring 70°, starting from the nose of the observer and extending downwards (Fig. 1b).

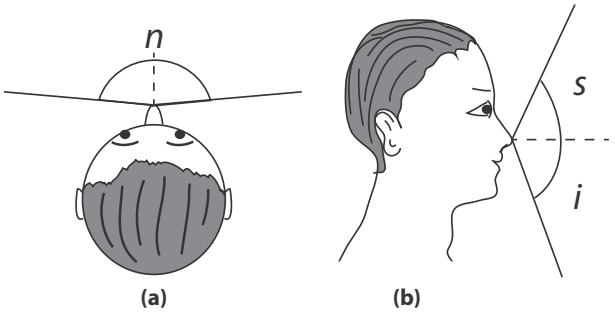


**Fig. 1.** The angles that define the static human FOV. (a) $n$ is the nasal angle defining a horizontal plane of 170° from the nose. (b) $s$ and $i$ are the superior and inferior angles defining lines extending 65° upwards and 70° downwards respectively from a horizontal line extending from the nose. When combined, these angles form an ellipse that defines the static FOV, shown in Fig. 2.

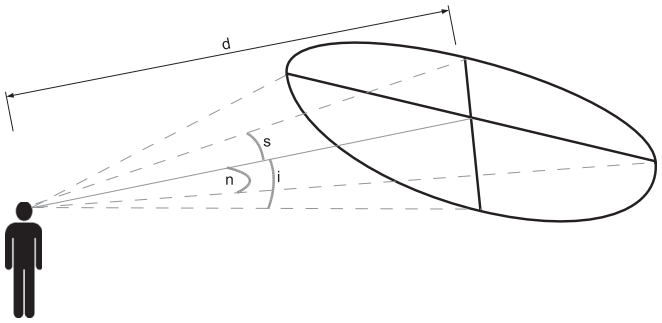


**Fig. 2.** The static field of view.

These angles define the region seen by at least one eye.

The virtual field of view area ($A_{fov}$) depends on the distance ($d$) between the observer and the object. The shape of the virtual field of view is an irregular ellipse of which the dimensions can be estimated by simple trigonometric relations.

Different values can be taken for angles $s$, $i$ and $n$ (e.g., considering only the full binocular part of the field of view, Spector, 1990). However, small changes to the values of these angles would cause only general scaling of the results without altering their meaning and the ratio between them.

If we now take into account the ability of the observer to move about a fixed point, we introduce two types of "dynamic field of view": "cylindrical" and "spherical".

In the first case, the observer can rotate their sight by 360° on the horizontal plane. Consequently, the elliptical shape of the field of view becomes the internal (lateral) area of a cylinder (Fig. 3).

In the second case, we extend this idea by assuming that the observer is able to move their sight in a vertical direction. The area of the field of view then becomes the internal area of a sphere (Fig. 4).

As photovoltaic panels generally have a low/flat profile, the dynamic cylindrical FOV approach is used to calculate their visual impact. Whereas, the vertical dimension of wind turbines is not negligible and thus the dynamic spherical FOV approach is applied to calculate their visual impact.

### *The perceived shape and size of an object*

The *perceived* size and shape of an object will differ from its *true* dimensions depending on the position (distance and angle) between the object and the observer. In the section Perceived size of an object, we demonstrate how the perceived size of an object is calculated. In the section Perceived size as a proportion of area of field of view, we demonstrate that when the perceived size is represented as the proportion of the field of view occupied by an object, this becomes independent of the distance between the observer and the object. This allows us to

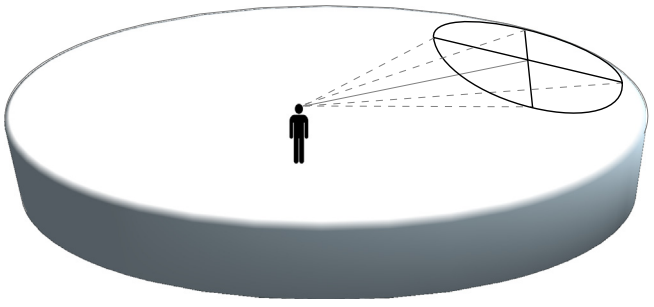

**Fig. 3.** The dynamic cylindrical field of view.

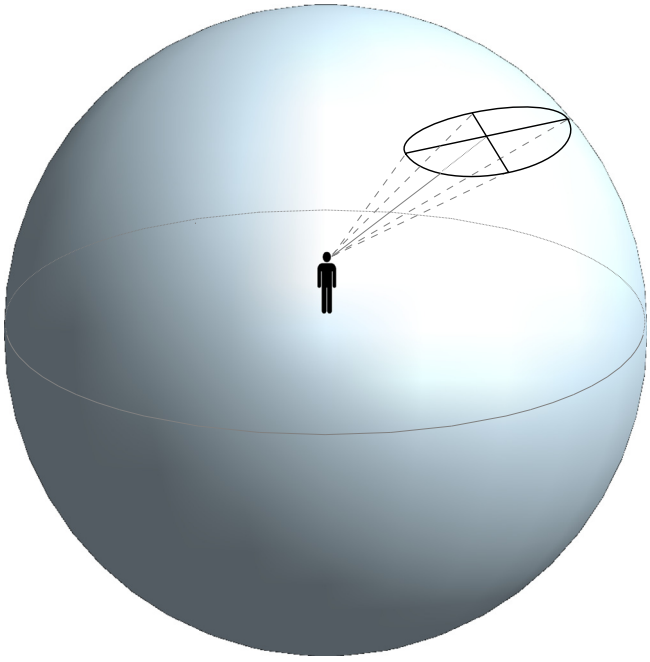

**Fig. 4.** The dynamic spherical field of view.

combine multiple objects at different distances to calculate the overall visual obstruction (outlined in the section Combining multiple objects at various distances). The sections Perceived size of an object to Combining multiple objects at various distances, principally discuss these calculations applied to a simple geometric shape. In the section Calculating perceived size of complex shapes, we explain how the true shape of wind turbines and photovoltaic panels can be simplified into a set of geometric shapes so these calculations can be applied.

*Perceived size of an object*

In Fig. 5a we show how the dimensions of an object vary depending on the position of the observer. The observer is looking at a straight black pole with a "true" height ($L$) and "true" diameter ($W$). The observer is at an oblique angle ($\alpha$) and distance ($p$) from the pole. In this example, the projective plane ($A_{fov}$) is centred on the pole at distance $d$ (in this case, $d = p$). The perceived area of the object ($l_a$) is equal to the perceived length ($l$) × perceived width ($w$).

The degree to which the perceived area of the object is distorted from the "true" dimensions is dependent upon:

- the angle ($\alpha$); the greater the angle between the observer and the pole, the smaller the perceived length ($l$) and consequently, the perceived area ($l \times w = l_a$). In particular when $\alpha = 0$, then $l = L$ and when $\alpha = 90$, then $l = w$.
- the distance ($p$); the greater the distance between the observer and the centre of the pole, the smaller the object appears relative to the FOV (i.e., the ratio $l_a/A_{fov}$).

*Perceived size as a proportion of area of field of view*

We can represent the perceived size of an object ($l_a$) as a proportion of the area of the field of view ($A_{fov}$), making a dimensionless measure $l_a/A_{fov}$. This is shown in Fig. 5b, where all variables are the same as Fig. 5a apart from the distance between the observer and the projective plane ($d'$) (i.e., the observer is focusing at a shorter distance). Although the perceived length of the pole ($l'$) is now shorter, the area of the field of view ($A'_{fov}$) is now smaller, and thus the ratio between the perceived area ($l'_a$) and the area of the field of view remains the same. Hence at a distance $d' \neq d$ we obtain that:

$$l'_a/A'_{fov} = l/A_{fov}. \quad (1)$$

*Combining multiple objects at various distances*

By measuring the perceived size of an object ($l_a$) as a proportion of the area of the field of view ($A_{fov}$) we can place the dynamic field of

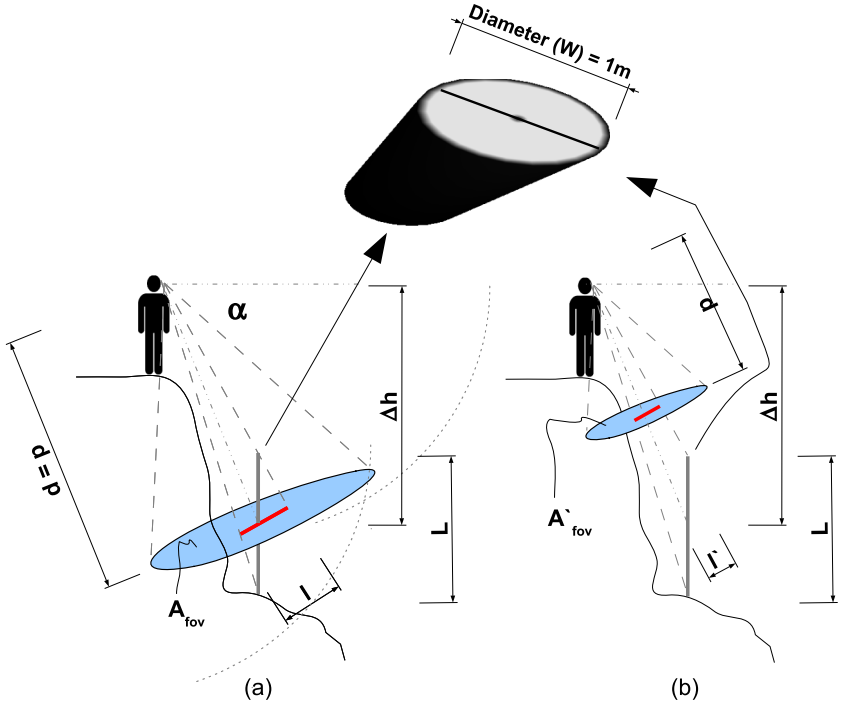


**Fig. 5.** Change in perceived height ($l$) of an object with different placements of the projective plane ($A_{fov}$). (a) The projective plane is centred on the object at distance $d$. (b) The projective plane is at a shorter distance, $d'$. Projective plane is denoted in light blue and perceived height in red. In both cases, the true dimensions of the object ($L \times W$) are the same and the observer is at distance $p$, angle $\alpha$ from the object. (For interpretation of the references to colour in this figure legend, the reader is referred to the web version of this article.)

view at an "arbitrary" distance ($d$). This allows calculation of the perceived size of multiple objects which differ in distance from the observer ($p$). Fig. 6 demonstrates this concept using the spherical dynamic field to estimate the observed areas ($l_{a1}$ and $l_{a2}$) of two different objects. We then calculate the overall dynamic field of view obstruction as a cumulative effect of the visual obstruction of individual objects. Hence, in general:

$$\sum_{i=1}^{n} l_{ai}/A_{sfov} \tag{2}$$

where $n$ is the number of objects, $lai$ is the observed area and $A_{sfov}$ is the spherical dynamic field of view at a fixed distance $d$ (arbitrarily chosen).

*Calculating perceived size of complex shapes*

The calculations in sections Perceived size of an object to Combining multiple objects at various distances were applied to a simplistic example of a straight pole. Although the geometry of wind turbines and photovoltaic panels is more complex, most standard facilities can be simplified to sets of shapes and the same calculations applied.

A wind turbine can be split into two shapes: the tower can be represented as a trapezium and the rotor blades as a filled circle (which takes into account the rotation of the blades). For simplification, the rotor blades are assumed to always be facing towards the observer (resulting in some overestimation of size from certain angles). As an observer moves closer to the wind turbine, the perceived shape of the rotor approaches a flattened ellipse (in the vertical dimension) (Fig. 7). These two shapes are then projected, depending on the α angle and the distance $d$. The projected areas are then summed.

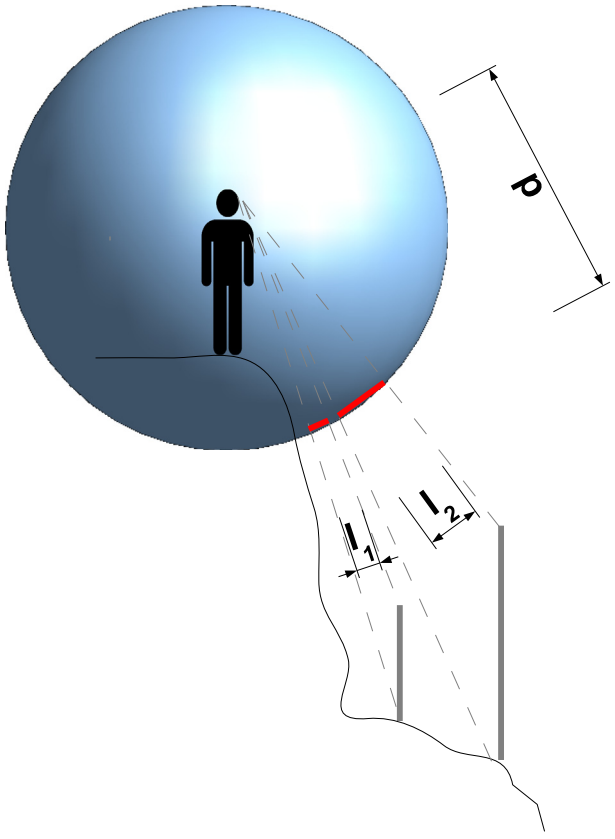


**Fig. 6.** Estimating perceived size and overall field of view obstruction of two different objects placed at different distances from the observer. A dynamic spherical field of view is used in the example.

**Fig. 7.** The observed geometry of an aerogenerator. The tower is represented as a trapezium and the rotor as a filled circle. Photo license: http://commons.wikimedia.org/wiki/File:Aerogenerator_No_5,_Drumderg_-_geograph.org.uk_-_1424342.jpg.

The observed shape of a photovoltaic panel is always a parallelogram or a trapezium. It is therefore easy to calculate its projected area (i.e., the obstruction of the field of view) by evaluating the two main projected dimensions (height and width) and then multiplying them (Fig. 8) to obtain the perceived area of the panel.

In previous studies, the shape of wind turbines and photovoltaic panels has been abstracted from simply the height and width of each element, which overestimates the proportion of field of view disturbed. Moreover, previous studies did not take into account the distortion of these shapes when viewing from different angles. We estimate that these inaccuracies in shape estimation cause an approximate doubling of the impact upon the field of view. By taking into account a more realistic shape and distortion, we believe that this method of visual impact quantification is more precise.

**Fig. 8.** The perceived shape of the photovoltaic panel. Photo license: http://commons.wikimedia.org/wiki/File:Panell_fotovolt%C3%A0ic.jpg.

*Visual impact index*

We quantitatively define the non-dimensional visual impact index (*NI*) as the ratio of the two areas:

$$NI = A_{obj}/A_{fov} \quad (3)$$

where:

$A_{fov}$ is the area of the chosen field of view (fixed, cylindrical or spherical);
$A_{obj}$ is the perceived area of the elements (photovoltaic panel or wind turbine).

When the observer can see multiple objects from one position, each object has a different distance ($p$) from the observer. However, the NI-index is independent of the distance between the observer and the projective plane ($d$) (section Perceived size as a proportion of area of field of view). Consequently, $d$ can be set to the distance between the observer and the nearest object. Then the other objects must be projected (dimensionally scaled using simple proportions) onto the same projective surface ($A_{fov}$). The total NI-index can be then calculated as the sum of all the NI-indices obtained from the different objects.

This index represents the percentage of impact (visual obstruction) produced by each single object in the field of view. In probabilistic terms, it represents the probability of visual impact from each single observation point: the ratio between positive events (when visual impact occurs) and all possible events.

*Calculation*

*r.wind.sun* is a Python script for GRASS GIS which evaluates the visual impact index (NI-index) for each cell of a raster map in the area surrounding one or more wind turbines or photovoltaic panels.

Required inputs are:

- a digital elevation model (DEM);
- a vector point map giving the location of centroids of the wind turbines or photovoltaic panels;
- dimensions and inclination of the facilities;
- distance threshold parameters to define the zone of analysis.

*Implementation for wind turbines*

For each facility, the perceived area is calculated for all cells in a given radius around that facility. The radius is defined by the user as a "maximum distance" parameter. For each pixel within the radius, the dynamic spherical field of view ($A_{fov}$) is calculated where $d$ is set to the minimum distance between that cell and the nearest wind turbine.

The r.wind.sun tool is able to take into account the impact of terrain morphology obscuring parts of each wind turbine. The tool schematically considers whether (i) only the upper half of the rotor is visible, (ii) the entire rotor is visible, and (iii) the entire plant is visible. If the entire plant is visible, the tool estimates the sum of the perceived area of the rotor and of the tower to evaluate the perceived area of the wind turbine. If the tower or part of the rotor is obscured by the terrain, the perceived area is calculated as half of the perceived area of the rotor.

*Implementation for photovoltaic panels*

For the photovoltaic panels, the tool calculates the perceived area for all cells that lie within a "donut" shape centred about the facility, defined by minimum and maximum distance threshold parameters. The minimum distance parameter is used to avoid analysis being performed upon the facility itself, or in neighbouring cells also containing photovoltaic panels (as they tend to be grouped together). To calculate the perceived area of each facility, the tool uses a cylindrical dynamic field of view where $d$ is equal to the distance from the nearest panel centroid.

*Processing*

From an algorithmic point of view, the analysis is performed sequentially upon each individual element (e.g., each single wind turbine). For each element, an individual raster map of the NI-index is generated. These maps are then summed together to obtain a final NI-index map for all facilities.

As the model is raster based, the processing time is strongly linked to the cell size and the maximum distance chosen to evaluate the visual impact (i.e., the size of the study region). Large values of the maximum distance and high spatial resolution strongly increase the processing time.

This has been an issue for raster analysis since the 1990s (Kinder et al., 1997). However, advances in software and technologies such as the optimization of algorithms have helped significantly in reducing the duration of the analyses. For example, on using a computer with 4 Gb of RAM and a 2.0 GHz processor running a Linux Operating System, applying the code to a study region with a maximum distance of 10 km from the facilities and a resolution of 10 m (more than 3 million cells), the analysis is completed in approximately 10 min. Moreover, the code could be parallelized in a way that GRASS GIS can process each wind turbine or panel in a different mapset.

*Output*

The main output of the r.wind.sun tool is a raster layer where the cell values represent the non-dimensional visual impact index (*NI*) value. There are various options for more detailed output from the tool. For example, if the user requires a three-dimensional view of the wind turbine, they can input a template (in.dxf format) of the facilities.

The values obtained for the impact index are often very small. Using the example of Fig. 5a and b, it is clear that an increase of $d$ (the distance from the projective plane), whilst maintaining a constant angle $\alpha$, does not result in large variations in $I_a$. However, it results in a substantial increase in $A_{fov}$. In our opinion, this is correct as it reflects the intuitive experience that an object apparently and rapidly "becomes small" when we move away from it.

Detailed practical steps for installing and executing the tool are outlined in Appendices 1–3.

## Case studies

We have tested the model using both synthetic (section Synthetic case study) and real data (section Real world application: Cima Mutali). The first application with synthetic data aims to explore the distortion effect in the quantification of visibility. The second experiment then demonstrates the tool function in a real setting.

*Synthetic case study*

In this section we show a synthetic example of how r.wind.sun is able to take into account the effect of the perceived size of objects on the visual impact index. To accomplish this task we will show how this effect can influence the estimation of the maximum distance at which an object is visible and, as a consequence the landscape area affected by the visual impact.

Molina-Ruiz et al. (2011) define a method to quantify the maximum visible distance for a tall linear object (suitable for analysis of wind turbines but not photovoltaic panels). Rodrigues et al. (2010) report a development of this method which allows calculation of maximum visible distance using a simplified (rectangular) area of the observed object.

The literature review did not reveal any papers that considered the effect of distortion of the shape and size of the observed object on the estimation of its visual impact. So it is useful to use r.wind.sun to show how the visual impact of a wind turbine can be affected by the possibly altered shape perceived by an observer.

We can define the minimum resolvable size of an object at various distances by a 25 arc minute$^2$ solid angle (Shang and Bishop, 2000).

Rodrigues et al. (2010) state that the maximum distance at which the object remains visible can be expressed as:

$$\Delta = \sqrt{\frac{I^w * I^h * c}{25}} = \sqrt{\frac{A_{obj} * c}{25}} \quad (4)$$

where:

$\Delta$ is the maximum visible distance in metres;
$I^{w,h}$ are the "true" width and height of the observed object in metres;
$A_{obj}$ is the "true" area of the observed object in square metres;
$c$ is a constant which converts steradians to square minutes:

$$c = (180 * 60/\pi)^2 \simeq 1.18 * 10^7. \quad (5)$$

At distance $\Delta$, for a well defined wind turbine or photovoltaic panel, it is possible to estimate the theoretical value of the NI-index, that we define as $TNI_\Delta = A_{obj}/A_{fov\Delta}$, where $A_{fov\Delta}$ is the area of the spherical or cylindrical field of view. This value can then be compared with that calculated using r.wind.sun ($NI_\Delta$). In this case we compare the NI-values starting from distances, because as this is the most influencing variable on the NI-index calculation, the distance affects directly the final index value. However, comparing the two index values (the theoretical and that produced through r.wind.sun calculation at the same distance $\Delta$) we can demonstrate that the r.wind.sun tool is able to take into account the effect of the perceived shape on the visual impact estimation.

The procedure to achieve this comparison is described in the flowchart in Fig. 9 and it is principally composed of the following steps:

1. knowing the area (size) of the observed object, the maximum distance value ($\Delta$) can be calculated using Eq. (5).
2. using $\Delta$ as the r.wind.sun "maximum distance", it is possible to run r.wind.sun and calculate the NI-index map.
3. the values of the NI-index map at distance $\Delta$, $NI_\Delta$, can be compared with the theoretical values ($TNI_\Delta$).

To avoid any effects of partial obscuration of objects due to topography, two very simplistic synthetic topographies were created: one perfectly planar and the other very schematically mountainous. We acknowledge that the example is extreme and very artificial but it is used to demonstrate the capability of the model to calculate the effects of distortion of objects, and therefore should be considered only as a technical exemplification.

Applying this approach to a planar area and thus observing the object frontally (meaning, not considering the effect of optical distortion on the object perception) the tool r.wind.sun verifies Eq. (5). The NI-index value obtained by the tool at $\Delta$ distance ($NI_\Delta$), is almost the same as that calculated theoretically ($TNI_\Delta$). In Fig. 10, we show an example of the results obtained modelling a 100 m high wind turbine on planar topography. The total area of the aerogenerator (considering the rotor) is 10,380.9 m$^2$. Following the previous steps:

1. the $\Delta$ distance is 6999.8 m ~ 7 km.
2. the NI-index map obtained through r.wind.sun is shown in Fig. 10a.
3. the theoretical NI-index value ($TNI_\Delta$) at the $\Delta$ distance is $1.68 \times 10^{-5}$, which means that the 0.00168% of the observer's spherical field of view is occupied by the wind turbine. Reading the map obtained using r.wind.sun, it can be verified that the impact value $NI_\Delta$ obtained at the $\Delta$ distance is equal to the $TNI_\Delta$ value (see Fig. 10b).

Next we introduce a regular slope (30° - Fig. 11a) in the topography to demonstrate the effect of perspective in evaluation of visual impact. Although the topography simulated in the example is very synthetic, it demonstrates the principle whilst removing and confounding factors caused by topography.

In this case, we expect that the r.wind.sun NI-index equals the theoretical $TNI_\Delta$ at a distance $\Delta_m \ll \Delta_h$ where $\Delta_h = \Delta^*\cos(30)$.

In Fig. 11 we show an example of the results obtained by modelling a 100 m high wind turbine and assuming a topography with a constant downward slope of 30° starting from the wind turbine. Following the previous steps:

1. the $\Delta$ distance remains 7 km but since it is inclined by 30°, corresponds to 6.06 km ($\Delta_h$) in terms of horizontal distance.
2. a new NI-index map is generated using r.wind.sun and showed in Fig. 11a.
3. the theoretical NI-index value ($TNI_\Delta$) at the distance $\Delta_h$ remains the same as before (since the inclined 3D distance is 7 km as for the planar topography). However, in the map obtained using r.wind.sun, the NI-index value at the $\Delta_h$ distance is substantially lower: $NI_\Delta \sim 1.38 \times 10^{-5}$.

Moreover, analysing the NI-index map produced by the r.wind.sun module, we found that it is possible to verify that the theoretical $TNI_\Delta$ value is achieved at a horizontal distance $\Delta_m \sim 5600$ m (Fig. 11b). $\Delta_m$ was obtained by filtering the NI-index map in order to remove all the values less than $TNI_{\Delta h}$ and then measuring the maximum distance between the wind turbine and the remaining cells in the filtered NI-index map.

The described results demonstrate that the r.wind.sun tool is able to take into account the effect of the perceived size on the visual impact.

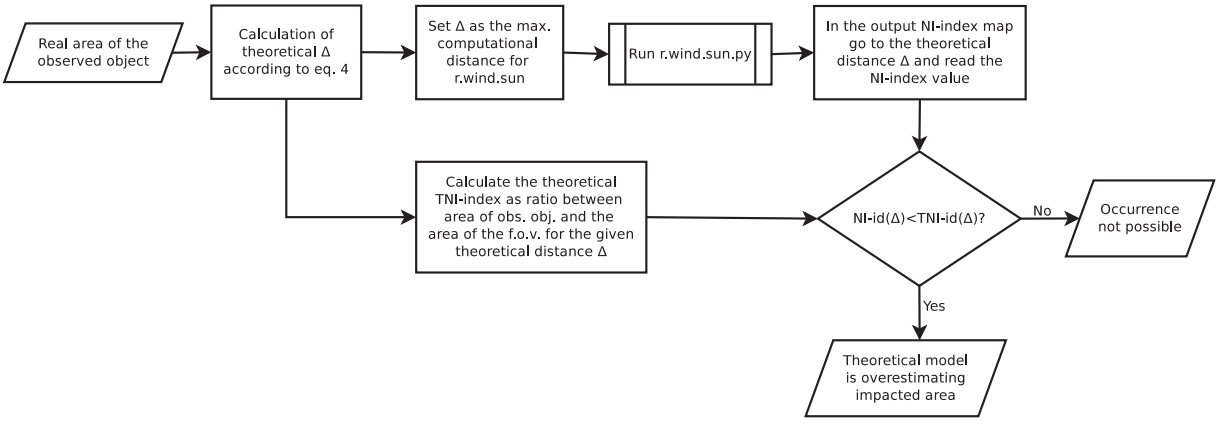


**Fig. 9.** Flowchart of the comparison procedure.

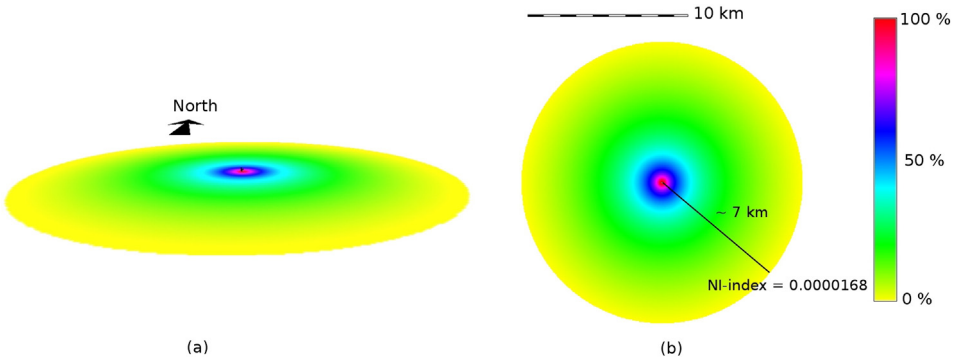


**Fig. 10.** NI-index map obtained using r.wind.sun to model the aerogenerator visibility on a flat terrain. (a) 3D and (b) 2D views of the results.

Using simple GRASS GIS tools, it is possible to evaluate the circular area (circular crown) between the theoretical and practical distances considered (5.6 km and 6.06 km). This area represents an exact measure of "how much" the effect of the altered perceived size affects the estimation of the visual impact. In the above example this area is estimated to be ~16.9 $km^2$, i.e., 14.7% of the area that should be considered visually offended not considering the effective of perspective.

We believe that these considerations are useful for the practical applications of the tool such as landscape planning.

*Real world application: Cima Mutali*

The tool was applied to two existing wind turbines, sited in "Cima Mutali", Fossato di Vico, Perugia, Italy. The NI-impact output map is shown in Fig. 12(left side).

Fig. 12(right side) shows the NI-index map reclassified into 6 bands (where bands are equal size intervals). A value of 1 denotes low impact, and the value of 6 denotes maximum impact. The 3D image (Fig. 13) of the reclassified impact map demonstrates how the tool is able to take into account the effect of the morphology in the partial obscuring of wind turbines.

In the zoom box in Fig. 13 we show that the NI-impact values increase from 1 to 6 (from yellow to red) as we move closer to the wind turbines. Areas with no colour denote zones where the wind turbines are not visible. There is a slight anomaly at the foot of the hill where visual impact actually decreases from 2 to 4 as we move towards the wind turbines. This is attributable to the fact that the hill only partially obstructs the wind turbines.

*Intuitive measures of visual impact for decision makers*

The absolute values of the NI-index are not immediately understandable or intuitive. In this section, we describe a method to create a comparative scale which could be used to communicate the results of the model to decision makers and landscape planners.

To do this, we take a small object of known dimensions (in this example, an ISO A4 sheet of paper) and calculate at what distance ($d_{A4}$) the piece of paper would have to be placed from the observer to create the same visual obstruction as the wind turbine. This can be done by recalculating the value of each single pixel of the output layer:

$$d_{A4} = \sqrt{\frac{A_{A4}}{4\pi * NI}} \tag{6}$$

where $NI$ = impact index, $A_{A4}$ = area of an A4 paper.

We believe that this method creates a more intuitive interpretation of the results and could be very useful for presenting to decision makers. In GRASS GIS this can be easily be performed using map algebra.

## Discussion and conclusions

To date, there is no precise set of rules to quantitatively (geometrically) estimate the visual impact of wind and photovoltaic farms. Perhaps because of this, often more prominence is given to other factors such as social or agricultural impacts (Cerroni and Venzi, 2009; Rogge et al., 2008). The tool we have developed here offers a more objective method to quantify this impact numerically, allowing direct comparison between sites and scenarios, providing a useful tool for landscape planners.

Similar tools exist to quantify the visual impact based on line-of-sight principles (e.g., Molina-Ruiz et al., 2011; Rodrigues et al., 2010). However, due to the r.wind.sun model taking into account the effects of (i) the real 3D distance between the observer and the object and (ii) the distortion of size and shape caused by the human eye in concurrence with the presence of a non-planar terrain morphology, the output

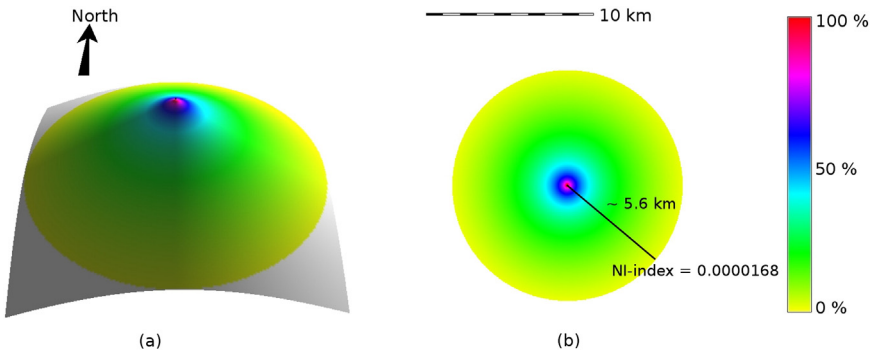


**Fig. 11.** NI-index map obtained using r.wind.sun to model the wind turbine visibility on a constant-slope terrain. (a) 3D and (b) 2D views of the results. The colour scale is logarithmic. (For interpretation of the references to colour in this figure legend, the reader is referred to the web version of this article.)

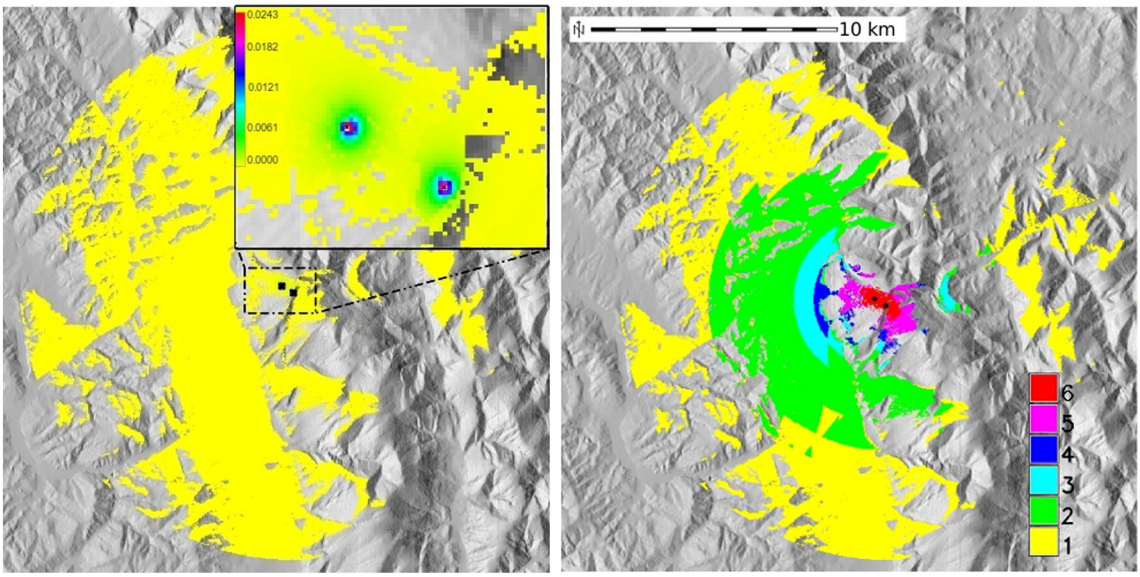


**Fig. 12.** Visual impact map for wind turbines in Cima Mutali, Central Italy. On the left: the NI-impact index value and (on the right) reclassification NI-impact into intensity bands: each band covers the same interval length of values.

of the r.wind.sun model can be considered more accurate calculations of visual impact.

These simpler formulations based only on the planar distance between the observer the object work well in the case of plain topographies but overestimate the visibility area in the case of different terrain morphologies. When applied to real cases (when the morphology is not typically planar and the possibility that the observer could view the plant from oblique angles), the maximum visible distance is overestimated by these simpler formulas. This is due to the effect of the morphology (which can hide or partially obscure facilities), and to the effect of distortion of the perceived area by the observer's eye.

Nonetheless, the perceived dimension of an object is only a part of the visual impact that an object can cause. For instance, colouring can play an important role in determining the visibility of an object (Bishop and Miller, 2007). In this sense the tool r.wind.sun can be considered a preliminary answer to the question of providing a quantitative estimate of the visual impact of wind turbines and photovoltaic panels.

The nondimensional nature of the tool developed here allows combination of results to more realistically simulate the visual impact of various facilities across a landscape (for instance, a combination of photovoltaic panels and wind turbines, or a large wind farm). Theoretically, this same approach could be used to estimate the visual impact of other major works/infrastructure in the same region (such as buildings, roads, quarries, and forests), assuming that it is possible to approximate their shape with simple geometrical models. This could bring a more integrated approach to the estimation of visual impact of man-made structures on a landscape.

## Appendix A. Supplementary data

Supplementary data to this article can be found online at http://dx.doi.org/10.1016/j.eiar.2014.07.002.

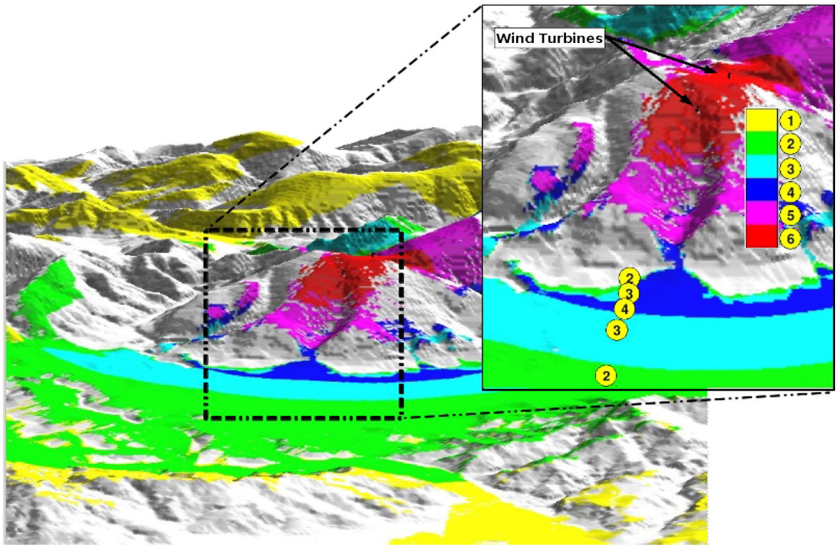


**Fig. 13.** Three-dimensional view of the territory of Fig. 12: the landscape and a detail. The 3D is produced using the GRASS GIS tool NVIZ. (For interpretation of the references to colour in this figure, the reader is referred to the web version of this article.)

## References


Bishop ID, Miller DR. Visual assessment of off-shore wind turbines: the influence of distance, contrast, movement and social variables. Renew Energy0960-1481 2007; 32(5):814–31. http://dx.doi.org/10.1016/j.renene.2006.03.009. [April].

Cerroni S, Venzi L. Confronto tra diverse localizzazioni di un impianto eolico contemperando produttività ed impatto visivo. Italia: Pubblicazioni Ce.S.E.T.; 2009 [0 URL: http://www.fupress.net/index.php/ceset/article/view/3225/2850. Access date 12 dec. 2012].

Chamberlain BC, Meitner MJ. A route-based visibility analysis for landscape management. Landsc Urban Plan0169-2046 2013;111:13–24. http://dx.doi.org/10.1016/j.landurbplan.2012.12.004. [March].

Chiabrando R, Fabrizio E, Garnero G. On the applicability of the visual impact assessment OAISPP tool to photovoltaic plants. Renew Sustain Energy Rev1364-0321 2011; 15(1):845–50. http://dx.doi.org/10.1016/j.rser.2010.09.030. [January].

Costella JP. Galilean antialiasing for virtual reality displays. sci.virtual-worlds. University of Melbourne; 1992 [preprint UM–P–92/105].

De Montis A, Caschilli S. Nuraghes and landscape planning: coupling viewshed with complex network analysis. Landsc Urban Plan0169-2046 2012;105(3):315–24. http://dx.doi.org/10.1016/j.landurbplan.2012.01.005. [15 April].

De Rubertis R. Fondamenti di geometria descrittiva. Roma: Edizioni Kappa; 1979.

Hurtado JP, Fernandez J, Parrondo JL, Blanco E. Spanish method of visual impact evaluation in wind farms. Renew Sustain Energy Rev 2003;8:483–91.

Ince DC, Hatton L, Graham-Cumming J. The case for open computer programs. Nature 2012. http://dx.doi.org/10.1038/nature10836.

Kinder RW, Rallings PJ, Ware JA. Parallel processing for terrain analysis in GIS: visibility as a case study. Geoinformatica 1997;1(2):183–207.

Ladenburg J. Visual impact assessment of offshore wind farms and prior experience. Appl Energy0306-2619 2009;86(3):380–7. http://dx.doi.org/10.1016/j.apenergy.2008.05.005. [March].

Landscape Institute. Environmental management assessment guidelines for landscape and visual impact assessment. 2nd ed. Spon Press; 2002.

Lewis NS, Nocera DG. Powering the planet: chemical challenges in solar energy utilisation. Proc Natl Acad Sci U S A 2006;103(43):15729–35. http://dx.doi.org/10.1073/pnas.0603395103.

Longely PA, Goodchild M, Maguire DJ, Rhind DW. Geographic information systems and science. 3rd ed. London: John Wiley & Sons; 2010.

Manchado C, Otero C, Gomez-Jauregui V, Arias R, Bruschi V, Cendrero A. Visibility analysis and visibility software for the optimisation of wind farm design. Renew Energy0960-1481 2013;60:388–401. http://dx.doi.org/10.1016/j.renene.2013.05.026. [December].

Moeller B. Changing wind-power landscapes: regional assessment of visual impact on land use and population in Northern Jutland, Denmark. Appl Energy0306-2619 2006;83(5):477–94. http://dx.doi.org/10.1016/j.apenergy.2005.04.004. [May].

Molina-Ruiz J, Martinez-Sanchéz MJ, Pérez-Sirvent C, Tudela-Serrano ML, Lorenzo MLG. Developing and applying a GIS-assisted approach to evaluate visual impact in wind farms. Renew Energy 2011;36(3):1125–32.

Neteler M, Mitasova H. Open source GIS: a GRASS GIS approach. The International Series in Engineering and Computer Science, vol. 773. New York: Springer 038735767X; 2008 [406 pp., 80 illus.].

Painuly JP. Barriers to renewable energy penetration: a framework for analysis. Renew Energy 2001;24(1):73–89.

Regione Autonoma Della Sardegna. Linee guida per l'individuazione degli impatti potenziali degli impianti fotovoltaici e loro corretto inserimento nel territorio (Guidelines for the assessment of the potential impacts of photovoltaic systems and for the correct siting). Decree n. 30/2 on the 23 May 2008; 2008.

Rodrigues M, Montanés C, Fueyo N. A method for the assessment of the visual impact caused by the large-scale deployment of renewable-energy facilities. Environ Impact Assess Rev0195-9255 2010;30(4):240–6. http://dx.doi.org/10.1016/j.eiar.2009.10.004. [July].

Rogge E, Nevens F, Gulink H. Reducing the visual impact of greenhouse parks in rural landscapes. Landsc Urban Plan 2008;87:76–83.

Scottish Natural Heritage, Scottish Renewables Forum, The Scottish Society of Directors of Planning. Visual representation of windfarms. Good practice guidance. http://www.snh.gov.uk/docs/A305436.pdf, 2006. [accessed 05.09.2013].

Shang H, Bishop ID. Visual thresholds for detection, recognition and visual impact in landscape settings. J Environ Psychol0272-4944 2000;20(2):125–40. http://dx.doi.org/10.1006/jevp.1999.0153. [June].

Spector RH. Visual fields. Clinical methods: the history, physical, and laboratory examinations. 3rd ed. Boston: Butterworths; 1990 [Chapter 116].

Toma L, Zhuang Y, Richard W, Metz M. r.viewshed tool. Geographical resource analysis support system (GRASS) GIS. Open Source Geospatial Foundation Project; 2012 [http://grass.osgeo.org/grass64/manuals/g.extension.html. Access date 13 dec. 2012].

Tsoutsos T, Tsouchlaraki A, Tsiropoulos M, Serpetsidakis M. Visual impact evaluation of a wind park in a Greek island. Appl Energy0306-2619 2009;86(4):546–53. http://dx.doi.org/10.1016/j.apenergy.2008.08.013. [April].

Turnbull WM, Gourlay I. Visual impact analysis: a case study of a computer-based system. Comput Aided Des0010-4485 1987;19(4):197–202. http://dx.doi.org/10.1016/0010-4485(87)90069-8. [May].

Van Rossum G, Drake FL. Python reference manual. Virginia, USA: PythonLabs; 2001 [Available at http://www.python.org. Access date 12 dec. 2012].

Vissering J, Sinclair M, Margolis A. A visual impact assessment process for wind energy projects. State clean energy program guide. CESA; 2011 [http://www.cleanenergystates.org/assets/2011-Files/States-Advancing-Wind-2/CESA-Visual-Impacts-Methodology-May2011.pdf accessed 06.09.2013].

Wüstenhagen R, Wolsink M, Bürer MJ. Social acceptance of renewable energy innovation: an introduction to the concept. Energy Policy 2007;35(5):2683–91. http://dx.doi.org/10.1016/j.enpol.2006.12.001.